HHS Public Access

Author manuscript

Exp Eye Res. Author manuscript; available in PMC 2019 June 01.

Published in final edited form as:

Exp Eye Res. 2018 June ; 171: 131–141. doi:10.1016/j.exer.2018.03.018.

Differences in α-Crystallin isomerization reveal the activity of protein isoaspartyl methyltransferase (PIMT) in the nucleus and cortex of human lenses

Yana A. Lyon, **Georgette M. Sabbah**, and **Ryan R. Julian**

Department of Chemistry, University of California, Riverside, 501 Big Springs Road, Riverside, CA 92521, USA, (951) 827-3959

Abstract

Although it is well-known that protein turnover essentially stops in mature lens fiber cells, mapping out the ensuing protein degradation and its effects on lens function over time remains challenging. In particular, isomerization is a common, spontaneous post-translational modification that occurs over long timescales and generates products invisible to most analytical methods. Nevertheless, isomerization can significantly impact protein structure, function, and solubility, which are all necessary to maintain clarity and proper refractive index within the lens. Herein, we examine the degree of isomerization occurring in crystallin proteins in the human eye lens as a function of both age and location within the lens. A novel mass spectrometric technique leveraging radical chemistry enables detailed characterization of proteins extracted from the cortex and nucleus of the lens. It is observed that the degree of isomerization increases significantly between the cortex and nucleus and between water-soluble and water-insoluble fractions. Interestingly, the abundance of L-isoAsp is low in the water-soluble cortex despite being the dominant product generated by isomerization of Asp in vitro, suggesting that Protein L-isoaspartyl methyltransferase (PIMT) is active in the cortex and suppresses the accumulation of L-isoAsp. The abundance of L-isoAsp increases dramatically in the nucleus, revealing that PIMT activity decreases over time in the center of the lens. In addition, the growth of L-isoAsp in the nuclear fraction suggests protein isomerization continues within the nucleus, despite the fact that most of the protein within the nucleus has become insoluble. Additionally, it is demonstrated that sequential Asp residues lead to isomerization hotspots in human crystallin proteins and that the isomerization profiles for αA and αB crystallin are notably different. Although αA is more prone to isomerization, αB loses solubility more rapidly upon modification. These differences are likely related to the distribution of Asp residues within αA and αB, which are in turn connected to refractive index. The high Asp content of αA is a hazard in terms of isomerization and aging, but it serves to enhance the refractive index of αA relative αB, and may explain why αA is only found in the eye.

Correspondence: ryan.julian@ucr.edu.

Keywords

Mass Spectrometry; Epimerization; Protein isoaspartyl methyltransferase; Long-lived proteins; Refractive Index

1. Introduction

Proteins within the human lens help provide the requisite refractive index needed for sight and inhibit molecular aggregation to particle sizes capable of scattering light (Horwitz et al., 1998; Rao et al., 1995). Given the lack of organelles within mature lens fiber cells, these functions must be performed in the absence of significant protein renewal or turnover (Samuel Zigler and Goosey, 1981). The proteins in the lens must therefore remain functional over significant lengths of time. The human lens also continues to grow throughout life, with newly synthesized cells continuously adding to the periphery (Augusteyn, 2007). Consequently, the approximate age of proteins within the lens is determined by their spatial location. The oldest proteins will be located in the central nucleus, while younger proteins will be found in the peripheral cortex. Crystallins constitute nearly 90% of the total water-soluble protein content in the lens fiber cells (Groenen et al., 1994). Protein degradation due to aging is thought to lead to loss of function in diseases such as cataracts and presbyopia, but complete characterization of all age-related protein post-translational modifications (PTMs) that might contribute to these maladies has proven elusive.

Among the major protein decay pathways, the mass-shifting PTMs in crystallins have been studied extensively, including disulfide bond formation, oxidation, phosphorylation, deamidation, and truncation (Ma et al., 1998). More subtle modifications such as epimerization and isomerization, which do not yield easily detectable mass-shifts, have received less attention. Epimerization is a specific type of isomerization that occurs when any single residue in a peptide converts from the L to D configuration at the alpha carbon position. Isomerization can also occur without affecting chirality, which in peptides occurs primarily through the formation of iso-aspartic acid (isoAsp). Importantly, recent work has suggested that, collectively, isomerization is the most prevalent class of PTM in the lens (Truscott and Friedrich, 2016). Although difficult to detect, isomerization significantly impacts protein integrity, contributing to loss of solubility and function by altering structure (Fujii et al., 2012, 2016; Lund et al., 1996; Masters et al., 1978) A study of α-crystallins in sheep lenses revealed that isomerization was highest in the disordered termini, which serve as intermolecular bridges in the formation of highly dynamic oligomers (Tao and Julian, 2014). It has also been shown that isomerization in the structured crystallin domain leads to reduced solubility (Lyon et al., 2017)

Aspartic acid is most susceptible to isomerization among the canonical amino acids, and asparagine can produce the same products via deamidation. The vulnerability of these residues is attributed to the susceptibility of the side-chain γ-carbonyl carbon to nucleophilic attack from the backbone nitrogen of the C-terminal amino acid (Fig. 1). The metastable L-succinimide ring thus formed can be hydrolyzed at one of two positions to form L-Asp or L-isoAsp. The increased acidity of the alpha-H in the succinimide ring also facilitates

racemization to form D-succinimide and subsequent hydrolysis yields either D-Asp or D-isoAsp. Over time, sequences containing L-Asp will spontaneously convert in four isomeric forms. Both of the isoAsp products reroute the protein backbone through the sidechain, which induces major perturbations in protein structure (Noguchi, 2010). Protein L-isoaspartyl methyltransferase (PIMT) is the only known repair enzyme for age-related Asp isomerization. PIMT is an *S*-adenosyl-L-methionine (SAM)-dependent enzyme that methylates L-isoAsp residues and D-Asp (700-10,000-fold lower affinity), allowing partial reformation of the L-Asp form (Lowenson and Clarke, 1992; McFadden and Clarke, 1987). Gene knock-out studies have shown that PIMT-deficient mice exhibit a nine-fold increase of L-isoAsp in the brain and die from epileptic seizures between 4 and 12 weeks (Qin et al., 2015; Yamamoto et al., 1998), while overexpression of PIMT in *Drosophila* increased lifespan by nearly 30% (Chavous et al., 2001).

Isomerization is an inherently difficult PTM to detect, as isomers have similar chemical properties and identical mass. Nevertheless, new gas-phase techniques involving both ion mobility spectrometry (IMS) and tandem mass spectrometry have been developed to tackle this problem. For example, D-amino acid containing peptides (DAACP) can be site-specifically detected by changes in drift time using ion mobility spectrometry coupled to mass spectrometry IMS-MS (Jia et al., 2014). Ultrahigh resolution IMS-MS can separate amyloid beta peptides containing all four aspartyl isomers (Zheng et al., 2017). Mass spectrometry-based techniques focus on discerning isomers by creating diagnostic fragments or comparing changes in fragmentation intensities. Electron capture dissociation (ECD) and electron transfer dissociation (ETD) can distinguish Asp from isoAsp through observation of unique mass c and z-type ions (O'Connor et al., 2006). In particular, radical-directed dissociation (RDD) has proven to be well-suited for isomer detection because it can be implemented in the analysis of semi-complex samples, such as the protein complement found in the lens. In RDD experiments, a radical is created site-specifically and is then activated to cause dissociation. The radical will migrate away from the initial site by pathways dictated by the three-dimensional peptide structure. Various side-chain and backbone fragments will be generated with isomer specific intensities, allowing for isomer identification in a high-throughput fashion (Tao et al., 2012). Thus, RDD enables full characterization of isomers and epimers, which are typically invisible to traditional proteomics.

Herein, the differences in isomerization from the cortex and nucleus of aged, human lenses are detailed. Prior to examination, the two regions of each lens were separated, and then further divided based on solubility. Enzymatic digestion was performed on each of the fractions and followed by tandem LC-MS using both collision-induced dissociation (CID) and RDD to distinguish isomers. Crystallin isomerization was studied as a function of age, and the results are analyzed in terms of location within the lens, sequence, tertiary structure, and PIMT activity. Additional experiments were carried out *in vitro* to establish the intrinsic isomerization propensities and influence of PIMT for comparison with the results obtained from the lens. The most important factors influencing age-induced isomerization are revealed and discussed in relation to maintenance of lens function.

2. Methods

2.1. Protein Extraction and Digestion

Human lenses were acquired from the National Disease Research Interchange (NDRI) (Philadelphia, Pennsylvania). Each lens was snap frozen and sent on dry ice overnight. Upon arrival, the samples were stored at −20°C until lens extraction was performed. The nuclei and cortices of the thawed lenses were separated using a 4mm trephine. The endcaps of each nucleus were removed by gently scraping off the outer tissue until only the dense, nuclear portion remained. The nucleus and cortex were then homogenized in 50mM Tris-HCl pH =7.8. The lens fractions were then centrifuged at 15,100g for 20 min at 4°C to separate the supernatant from the precipitate. The supernatant (water-soluble) was purified by dialysis against water. The precipitate (water-insoluble) was solubilized in 6 M urea and purified by dialysis against 6 M urea. For water-soluble digestion, 50 μg of protein was dissolved in 50 mM NH_4HCO_3 buffer, pH =7.8, disulfide bonds were then reduced with 1.5 μL of 100 mM DTT at 70°C for 10 minutes. After returning to room temperature, reduced cysteines were capped using 3 μL of 100 mM iodoacetamide in the dark for 20 minutes. Finally, the proteins were digested with trypsin for 12 hours at 37°C using a 50:1 protein to enzyme ratio. For the water-insoluble digestion, 100 μg of protein was dissolved using 6 M in 50 mM Tris-HCl, pH= 8.0. Disulfide bonds were reduced using 5 μL of 200 mM DTT in Tris-HCl, pH=8.0 at 37°C for 20 minutes. Following this, 20 μL of 200 mM iodoacetamide in Tris-HCl, pH= 8.0 was added, and the mixture was incubated in the dark for one hour. To consume unreacted iodoacetamide, 20 μL of 200 mM DTT was added and incubated for one hour in the dark. Next, the urea concentration was diluted to < 0.6 M using 50 mM Tris-HCl, 1 mM $CaCl_2$, pH= 7.6. The proteins were digested using trypsin with a 50:1 protein to enzyme ratio for 16 hours at 37°C. For the iodobenzoate modification, the digested peptides were desalted using a Michrom peptide trap (3 × 8 mm, C8) (Michrom Bioresource Inc). Approximately 5 nmoles of the digestion mixture, 10-100× excess of 4-iodobenzoic acid N-hydroxysuccinimide-activated ester in dioxane and borate buffer (pH =8.6) were combined and incubated for 1 hour at 37°C. Important: Dimethyl sulfoxide should not be substituted for dioxane in this step because it can cause aspartic acid isomerization. The modification side products at arginine and tyrosine side chains were removed by incubating the reaction mixture in 1 M hydroxylamine, pH= 8.5. The same procedure was used for the synthetic peptide standards. These procedures have been determined previously not to yield any detectable isomerization in control experiments (Tao and Julian, 2014).

2.2. Peptide and Radical Precursor Synthesis

All synthetic peptides were synthesized manually using standard FMOC SPPS procedures with Wang Resins as the solid support (Hood et al., 2008). N-hydroxysuccinimide (NHS) activated iodobenzoyl esters were synthesized by a previous procedure (Ly et al., 2011).

2.3. IQTGLDATHAER and IQTGLNATHAER Incubations

Synthetic model peptides were first purified using a Jupiter Proteo column (250 mm × 4.6 mm, 4 μm, 90 Å, C12) (Phenomenex, Torrence, CA). Following purification, 100 μL of 0.1mM model peptides were incubated in Tris-HCl, pH= 7.4 at 37°C for 22-43 days in parafilm-wrapped centrifuge tubes.

2.4. PIMT Experiments

Enzymatic methylation reactions were carried out in Tris-HCl pH= 7.4 at 37°C in a final volume of 50 μL containing 50 μM peptide substrate, 3.9 μM Protein isoaspartyl methyltransferase (Human, His tag, *E. coli*) (ATGen, Seongnam-si, South Korea), 400 μM S-5′-adenosyl-L-methionine (SAM) hydrochloride (Cayman Chemical, Ann Arbor, MI). Aliquots were sampled at 0, 0.45, 3, 6, and 24 hr. Reactions were quenched using 0.2% trifluoroacetic acid and stored at −20°C.

2.5. Mass Spectrometry and Radical Directed Dissociation

Solutions were analyzed using an LTQ linear ion trap mass spectrometer (Thermo Fisher Scientific, San Jose, CA) with a standard electrospray ionization source. The posterior plate of the ion trap was modified with a quartz window to allow fourth-harmonic (266 nm) laser pulses from a flash-pumped Nd:YAG laser (Continuum, Santa Clara, CA). Photodissociation (MS^2) of the *para*-iodobenzoate labeled peptide induces homolytic dissociation of the carbon-iodine bond producing a radical peptide. This is done using a digital delay generator (Berkeley Nucleonics, San Rafael, CA) which synchronizes laser pulses to irradiate the trapped ion cloud without supplemental collision energy. Further collision-induced dissociation (MS^3) was performed on the radical by re-isolation of the largest peak in the photodissociation spectrum.

2.6. LC-MS Data Acquisition and Analysis

An Agilent 1100 series HPLC system (Agilent, Santa Clara, CA) with a BetaBasic column (150 mm × 2.1 mm, 3 μm, 150 Å, C18) was coupled to an LTQ mass spectrometer. Peptides were separated using a 0.1% formic acid in water (mobile phase A) and a 0.1% formic acid in acetonitrile (mobile phase B) binary system at a flow rate of 0.2 mL/min. The digestion mixtures were loaded onto the column and separated using the following gradient: 5% B to 20% B over 60 minutes, 20% B to 30% B over the next 45 minutes, 30% B to 50% B over the next 15 minutes and 50% B to 95% B over the final 10 minutes. Another gradient of 3% B to 20% B over 80 minutes was also used to help separate a few coeluting peptides with very short retention times. The LTQ was operated in data-dependent mode using the Xcalibur program (Thermo Fisher Scientific). Specifically, in the CID-only LC-MS run, the first scan event was a full MS from m/z 300-2000 Da, followed by an ultrazoom (MS^2) and then CID (MS^3). In the RDD LC-MS experiments, the laser pulses were triggered during the MS^2 step and CID was performed as a pseudo-MS^3 step. Due to the high photodissociation yield of the 4-iodobenzoic acid chromophore, the major peak during this step is the loss of iodine, and it is the subsequent precursor for MS^3. The exclusion time was set to 60 seconds for the identification of peptides. For isomer identification, an inclusion mass list was added and the exclusion time was reduced to 16 seconds to enable repeated analysis of isomers. For both peptide and isomer identification, a rejection mass list of common mass spectrometry contaminants and interferences was applied to each experiment. Relative peptide isomer abundances were determined using the ICIS Peak Integration algorithm provided in Xcalibur and reported as the area of the single isomer peak over the cumulative area of each isomer.

MS data was acquired with Xcalibur software. The .raw files were converted to .mgf files using MSConvert software. The .mgf files were searched with X!Tandem PILEDRIVER edition (version 2015.04.01.1) against the *Homo sapiens* UniprotKB database. The cleavage sites were set as lysine and arginine (semi cleavage was turned on), allowing up to two missed cleavages and one point mutation). Carbamidomethylation (+57.02 Da at Cys) was set as a fixed modification, and N-acetylation, phosphorylation and oxidation were all considered as variable modifications. For the iodobenzoate-modified digestion mixture, the modifier (+230.01 Da) was considered as a possible modification at either the N-terminus or lysine side chain. The parent monoisotopic mass error was set to ±1 Da, the minimum parent mass was set to 300 Da and the fragment mass error was set to ±0.4 Da. The criteria for accepting peptides identified by X! Tandem was $e < 0.005$. The false discovery rate is, on average 1.9%, calculated using decoy sequences created by reverse database searching.

2.7. Calculation of R Values

To quantify isomer identification, R values were calculated, as originally described by Tao and co-workers (Tao et al., 2000). In this paper, R_{isomer} represents the ratios of the relative intensities of a pair of fragments that vary most between two isomers (R_A/R_B). Following acquisition of a tandem mass spectrum, R_{isomer} values are calculated for all pairs of peaks to reveal fragments that yield the best differentiation. If $R_{isomer} = 1$ then the two MS^n spectra are indistinguishable and the species are likely not isomers. If $R_{isomer} > 1$, a larger number indicates a higher probability that the two species are isomers. The relative intensity of the peaks used for the R_{isomer} score must be higher than 5% of the base peak in at least one of the spectra. To confidently identify each of these isomers by MS^n, we use a threshold that was determined by performing a *t*-Test on the R_{isomer} values obtained by performing CID and RDD on a mixture of synthetic peptides separated by LCMS. Using 99% confidence intervals, the R_{isomer} threshold for CID is >1.9 and for RDD it is >2.4 (Tao and Julian, 2014).

2.8. Calibration Curve for TVLDSGISEVR L-Asp/D-isoAsp Coelution

A calibration curve generated from the L-Asp and D-isoAsp standards was needed to quantify the relative abundance of these coeluting isomers from TVLDSGISEVR. Mixtures containing 0%, 25%, 50%, 75% and 100% of D-isoAsp were prepared and analyzed using the same LC-MS parameters for the digests. The y-axis represents the difference over the sum of the two peaks that had the largest differences in relative intensities in the fragmentation spectra of these two isomers. (Supplemental S1).

2.9. Protein Modeling

UCSF Chimera version 1.9 was used to generate the models used in Figs. 5 and 6 (Pettersen et al., 2004).

2.10. E91D Mutation of αA

The crystal structure of αA was obtained from PDB 3L1F, which reports the structure for the bovine protein where the residue in position 91 is a glutamic acid. In the human αA-crystallin, there is as conserved mutation placing an aspartic acid at this position. To show

the explicit location of the Asp91-Asp92 motif in αA from human, an E91D mutation was performed in silico. The αA mutant was then minimized using the OPLS3 force field in Maestro MacroModel version 10.5.014 (Schrodinger Inc., Portland, OR, USA)

3. Results

3.1. Changes in αA-crystallin isomerization profiles in aged human lenses

Fig. 2a illustrates LC chromatograms for Ac-MDVTIQHPWFK, the acetylated N-terminal peptide obtained by tryptic digestion of αA. 39-, 55- and 72-year-old lenses were sampled, and the results obtained from the water-insoluble (WI) fraction of the nucleus (the oldest proteins in the lens) are shown. To confirm the identities of the isomers, synthetic versions of the peptide containing L-Asp, L-isoAsp, D-Asp and D-isoAsp were synthesized. The fragmentation pattern of the peptides from the digest was compared to the standards, then R_{isomer} scores were used to confirm the exact identity of each isomer (Supplemental S2 and S3). The results indicate that the first Asp isomer to elute is L-isoAsp, followed by D-isoAsp, L-Asp and finally D-Asp. The relative amount of L-Asp decreases steadily as a function of age from 78 ± 4% in the 39-year-old lens to 45 ± 3% in the 72-year-old lens. D-isoAsp is the most abundant degradation isomer for all ages, though the proportion relative to L-isoAsp becomes nearly equivalent over time. Another product identified in the chromatograms corresponds to glutamine deamidation, denoted as Q→E. The three deamidated glutamine peaks may represent three different isomers of Glu or a combination of coeluting, isomerized Asp and Glu.

The results from Ac-MDVTIQHPWFK and other αA peptides are summarized in Fig. 2b by reporting the total percent isomerization. Additionally, the protein regions are labeled according to their respective structural domains. Although the overall trend illustrates isomerization increases with age, there are some regions where isomerization is nearly equivalent for all ages. ^{13}TLGPFYPSR^{21} from the N-terminal region (NTR) undergoes very little isomerization, while ^{146}IQTGLDATHAER^{157} from the C-terminal region (CTR) is already extensively isomerized in the youngest sample.

3.2. Changes in αA-crystallin isomerization between the cortex and nucleus

Fig. 3a shows LC chromatograms from Ac-MDVTIQHPWFK, comparing results obtained from the WS cortex, WI cortex, and WI nucleus of the 72-year-old lens. Although the fraction corresponding to the WS nucleus was also examined, it contained insufficient concentration of this peptide for analysis. The L-Asp isomer is dominant in the WS cortex. D-isomers are prevalent in the WI cortex, where L-isoAsp represents the lowest abundance isomer. For the WI nucleus, L-isoAsp increases dramatically, accounting for nearly 3× the abundance of D-Asp. The results from similar analyses of other peptides are summarized in Fig. 3b, where the total percent isomerization is reported. In general, a consistent trend is noted where the degree of isomerization increases from WS cortex to WI cortex to WI nucleus. For peptides where data from the WS nucleus was obtained, the degree of isomerization is either comparable to, or slightly below the level observed in the WI nucleus.

Although the total percent isomerization in Fig. 3b is useful for examining overall trends, detailed information about individual isomers is lost. More comprehensive data is provided in Fig. 3c, where the fractional percent of each isomer from the 72-year-old lens is illustrated in a stacked bar chart. The fractional percent isomerization for each isomer was determined by the peak areas from the LC chromatogram, e.g. the data shown in Fig. 3a. Isomers with confirmed identities are illustrated in gray (L-Asp), pink (L-isoAsp), teal (D-isoAsp), or green (D-Asp). Unidentified isomers are shown in muted pastel colors, and all isomers are ordered by elution times. Results for the N-terminal peptide, Ac-^{1}MDVTIQHPWFK^{11}, are shown in the lowest dataset grouping on the y-axis. The fractional percentages match the results shown in Fig. 3a. For many of the peptides, the L-Asp isomer is most abundant. However, if the peptide contains multiple Asp residues, it is more likely that an isomerized peptide will be most abundant. L-isoAsp is typically found in small quantities in the WS cortex but occupies a greater fraction of the total in the nucleus. Significant amounts of D-isomers are observed, particularly in the insoluble fractions.

3.3. In vitro versus in vivo isomerization of a model peptide from αA-Crystallin

The *in vivo* isomerization products for ^{146}IQTGLDATHAER^{157} as determined by LC are shown in Figs. 4a–d. L-isoAsp represents a very modest fraction of the total in both the WS and WI cortex fractions. In contrast, L-isoAsp is abundant in the nucleus, shifting from the least abundant isomer identified in the WI cortex to the second largest peak in the WI nucleus. Although the amount of D-isomers also increases in the nucleus, the rise of L-isoAsp is disproportionately large. The intrinsic isomerization tendencies of IQTGLDATHAER were evaluated by incubating synthetic L-Asp peptide at 37°C in Tris-HCl, pH 7.4. After 43 days, the L-Asp form still accounted for >80% of the peptide, with L-isoAsp representing the largest degradation product (see Fig. 4e). It is known that formation of the crucial succinimide intermediate is 13-35 times faster with replacement of Asp for Asn (Stephenson and Clarke, 1989). This substitution allows for more rapid determination of the propensity for ring-opening to the L-Asp isomer. After 22 days, 49% ±3% of the L-Asn peptide deamidated, yielding the results shown in Fig. 4f. L-isoAsp is the dominant product, in agreement with previous observations (Riggs et al., 2017), and only ~30% of the peptide returns to the L-Asp form. The deamidated product shown in Fig. 4f was then incubated with PIMT and SAM in Tris-HCl pH= 7.4 at 37°C. Fig. 4g shows the chromatogram after 45 minutes of incubation. The full mass spectrum on the bottom shows that the L-isoAsp peak contains three coeluting species: L-isoAsp, L-isoAsp methyl ester and the succinimide ring. Results obtained after 6 hours of incubation are shown in Fig. 4h, where the total relative amount of L-isoAsp has decreased to 2.5%. The L-Asp product increases from 32% to 77%, which is also accompanied by an increase in the amount of D-Asp and D-isoAsp.

3.4. Isomerization patterns for structurally similar α-Crystallins

LC chromatograms for ^{90}VQDDFVEIHGK^{100} from αA and ^{93}VLGDVIEVHGK^{103} from αB are shown in Fig. 5 along with relevant portions of the crystal structures containing these peptides. The native L-Asp isomers are labeled in each spectrum, but the remaining isomers are not identified because it is unfeasible to synthesize all possible standards for peptides with multiple Asp residues. It is also unlikely that all isomers will chromatographically resolve. To verify that the L-Asp peak does not contain multiple isomers, the CID spectra at

the front and the back end of the peak were compared using an R_{isomer} score. The R_{isomer} scores are 1.5 (WS cortex), 1.7 (WI cortex) and 2.3 (WI nucleus). The R_{isomer} score for the WI nucleus is above the threshold (>1.9), suggesting this peak contains coeluting isomers. The abundance of the L-Asp isomer decreases from 70.4% in the WS cortex to 31.4% in the WI cortex. Since the L-Asp peak of the WI nucleus contains another isomer that cannot be quantified, the amount of L-Asp cannot be specifically determined, but the entire peak comprises only 9.6% of the total, which represents an upper limit for the amount of L-Asp present. The crystal structure of αA shows that Asp91 and Asp92 are both located within a beta-hairpin (Fig. 5b). The higher order structure in αB is identical to αA in this region, with Asp96 of ^{93}VLGDVIEVHGK^{103} also residing in a beta-hairpin (Fig. 5c). Despite the structural similarities, the LC chromatograms show that ^{93}VLGDVIEVHGK^{103}, which contains a single Asp residue, is significantly less prone to isomerization (compare Fig. 5a and 5d).

Figures 6a, 6b, 6f, and 6g compare changes in the total % isomerization between αA and αB for the WI cortex and WI nucleus of a 72-year-old lens. Fig. 6c illustrates the sequences of the two proteins, color-coordinated by structural motif, with Asp and Ser residues denoted in black and acidic repeats in red. In Figures 6d and 6e, representative crystal structures for αA and αB are shown. Both proteins have similar structural motifs, but their primary sequences differ significantly. Human αA and αB share modest 57% sequence homology (Horwitz et al., 1999). Noticeable differences in the primary sequences include deviations in the aspartic acid content and location. In αA, there are 15 aspartic acids compared to 11 in αB. Unlike αA, αB does not contain any aspartic acids in the C-terminal tail and lacks any aspartic acid repeats. The isomerization profiles also differ substantially between proteins. In general, αB is less isomerized than αA, but isomerized peptides are more likely to remain soluble in αA than αB. For example, there are five isomerized peptides in αB that are only found in the WI fraction, including significantly degraded peptides such as ^{108}QDEHGFISR^{116}. In the WI fractions, αA is more degraded, particularly in the ordered alpha-crystallin domain (ACD).

4. Discussion

In general, our results agree with the well-known trend that epimerization and isomerization increase as a function of protein age (Fujii, 2005; Fujii et al., 2010), but interestingly, many individual peptides exhibit a weak change in isomerization over time. For example, many of the peptides in Fig. 2 are approximately 80% isomerized in all samples. Given that the succinimide intermediate always produces some of the native L-isomer, 80% isomerization likely is close to the expected equilibrium value. These highly isomerized peptides are found in both the disordered N-terminal and C-terminal regions and in the structured alpha-crystallin domain, suggesting that tertiary structure alone does not dictate isomerization rate. The most highly modified peptides contain multiple sites prone to isomerization (i.e. multiple Asp or Ser residues), which likely increases the probability for modification by enhancing local structural flexibility and the rate of succinimide formation (for Asp containing peptides). Interestingly, both of the highly degraded peptides observed in the ordered domain contain sequential Asp residues, which have previously been identified as isomerization hotspots (Lyon et al., 2017; Yi et al., 2013; Zhang et al., 2011). This

phenomenon is discussed in further detail below. In contrast, peptides lacking sequential Asp residues in the alpha-crystallin domain show steady increases in isomerization as a function of age, suggesting that tertiary structure can influence the rate of isomerization (even if it is not a completely dominant factor).

More consistent trends are found when the degree of isomerization is examined as a function of location within the lens, as illustrated in Fig. 3. Crystallins are typically water-soluble, but degradation can lead to loss of solubility, which becomes dominant in the nucleus around 40 years of age (McFall-Ngai et al., 1985). The nucleus is the oldest and most isolated part of the lens, while newly-synthesized proteins are continuously added to the cortex (Augusteyn, 2007). By separating the nucleus and cortex, proteins of different ages can be examined within a single lens from one person, allowing many variables to remain constant. The results in Fig. 3 illustrate a clear trend, with proteins from the WS cortex being least degraded, followed by the WI cortex, WS nucleus (when detectable), and finally the WI nucleus. Not surprisingly, the paucity of WS proteins in the nucleus limits detection of peptides from this fraction.

One of the most striking features of Fig. 3c is the limited amount of L-isoAsp detected in any peptide from the cortex. Although some increase in abundance is noted between the WS and WI cortical fractions, a more dramatic shift is always observed by comparing the cortex and nucleus. On average, the relative amount of L-isoAsp increases from 6.5% (WI cortex) to 17.5% (WI nucleus). No other isomers exhibit such a reproducible shift in abundance between these fractions. The regional activity of PIMT can explain these results. We detected PIMT in the cortex of the 39 and 55 y/o lenses, with each digest yielding 3-4 unique peptides and confident assignment of the protein. These results agree with McFadden and Clarke, who previously identified PIMT in human lenses (McFadden and Clarke, 1986). Additionally, they found PIMT activity decreased with increasing age, including a reduction in activity in the nucleus compared to the cortex. L-isoAsp is the primary target for PIMT (Griffith et al., 2001), and our results suggest that PIMT efficiently suppresses the accumulation of L-isoAsp in the cortex but is unable to effectively repair either D-isomer, in agreement with previous studies on substrate affinity (Johnson and Aswad, 1985; Murray and Clarke, 1984). The modest increase in L-isoAsp in the WI cortex suggests that PIMT cannot repair soluble and insoluble proteins with the same efficiency. Greater accumulation of L-isoAsp is also detected as a function of age in the WI nucleus (Fig. 2a). The relative amount of L-isoAsp in the 39 y/o nucleus was 2.8% but increased nearly 5× in the 55 y/o lens, which was dramatically greater than the increase in the D-isoAsp and D-Asp content. The significant jump in L-isoAsp in the WI nucleus has two important implications, 1) PIMT has lost significant activity in the nucleus for adults over ~40-years-old, and 2) isomerization continues to occur in the nucleus after loss of PIMT activity. If proteins in the nucleus remained static after the loss of PIMT activity, then an increase in the abundance of L-isoAsp would not be expected.

Further support for the role of PIMT is provided in Fig. 4g,h. Shortly after addition of PIMT and SAM to the peptide mixture shown in Fig. 4f, preferential modification of L-isoAsp is detected (Fig. 4g). Both the succinimide and methylated versions of the peptide have different masses and are easily distinguished by MS. After 6 hours of incubation, the relative

amount of L-isoAsp decreases from 57% to 2.5% (Fig. 4h). While the L-Asp product increases from 32% to 77%, also accompanied by increases in D-Asp and D-isoAsp. PIMT does not directly produce L-Asp, it merely methylates L-isoAsp, which facilitates reformation of the succinimide ring. All four isomers are produced upon ring-opening, but the L-isoAsp will be methylated again. Eventually, this cycle drives down the population of L-isoAsp and also increases the abundance of L-Asp and D-isomers. These *in vitro* results are consistent with the isomer populations observed in the WS fractions from the cortex and suggest that PIMT is responsible for suppression of L-isoAsp in the younger portions of the lens. These results suggest that PIMT serves to prolong the timescale over which crystallin degradation occurs, delaying loss of solubility and subsequent aggregation that may eventually lead to cataract formation.

Previous experiments have demonstrated that sequential aspartic acid residues lead to isomerization hotspots (Lyon et al., 2017; Yi et al., 2013; Zhang et al., 2011). Aspartic acid hotspots may also occur following deamidation of Asn in the “ND” or “DN” motifs that are found in γS and βA1, respectively (Hooi et al., 2012). It is known that PIMT repair of L-isoAsp is hampered if the n+1, n+2 or n+3 residue is acidic, which would contribute to the hotspot effect (Lowenson and Clarke, 1991). However, other contributing factors, such as increased backbone flexibility may also be important but have not been tested. The results in Fig. 5 reveal additional insight into the nature of isomerization hotspots resulting from sequential Asp residues. Evaluation of peptides from αA and αB that adopt identical secondary structure within the ordered ACD and are comprised of similar sequences reveals a remarkable difference in isomerization. Importantly, ^{88}VQDDFVEIHGK^{98} (from αA) is highly isomerized in all fractions, yet ^{93}VLGDVIEVHGK^{103} (from αB) is significantly less modified. This confirms that the hotspot effect due to sequential Asp residues observed previously in ~1-year-old lenses from animals is also relevant in humans. Furthermore, hotspot isomerization does not result in a simple doubling of normal isomerization since the amount of modification in ^{88}VQDDFVEIHGK^{98} is not twice that in ^{93}VLGDVIEVHGK^{103}. Furthermore, the presence of Glu99 should inhibit PIMT, suggesting that the hotspot effect is not solely a consequence of reduced enzymatic repair. Given the susceptibility of consecutive Asp residues to age-related isomerization, why are such sequences found in αA?

The answer may be surmised after further comparison of αA and αB as shown in Fig. 6. Although the ordered structures are nearly indistinguishable (Figs. 6d and 6e), the sequences (Fig. 6c) vary significantly in Asp content and distribution. As a consequence, the isomerization profiles of αA and αB are strikingly different, compare Fig. 6a versus 6b and Fig. 6f versus 6g. Close inspection reveals that αB does not contain any sequential Asp residues and therefore does not contain any Asp-Asp hotspots. The disordered C-terminal domain of αB also lacks Asp, making it less susceptible to isomerization. Overall, isomerization in αB appears to drive protein insolubility to a greater extent than αA, as noted by the paucity of isomerization in the WS cortex (Fig. 6b, upper). Collectively, αB is less susceptible to isomerization, begging the question, why is αA needed? Knockout studies in mice revealed normal development without αB but not without αA, which led to premature cataract formation. Furthermore, the chaperone activity of α-crystallin is highest with a ratio of 3:1 αA to αB, suggesting that a combination of the two proteins may be

optimal (Srinivas et al., 2010). Although αA is more prone to isomerize, it differs from αB in another important respect, refractive index. Asp is one of the key amino acids required to increase the refractive index of a protein (Glu is not) (Zhao et al., 2011). The increased balance of Asp rather than Glu within αA contributes to its greater refractive index increment (0.1938 αA, 0.1922 αB, d*n*/d*c* (ml/g)). The liability of Asp incorporation into αA in terms of susceptibility to isomerization over time appears to be outweighed by the need for greater refractive index.

There are also notable differences in the location of serine residues between αA and αB, particularly in the alpha-crystallin domain. ^{11}RPFFPHSPSR^{21} from the N-terminal region of αB is significantly more epimerized than the corresponding peptide in αA. RDD identified three isomers of ^{11}RPFFPHSPSR^{21} as shown in (Supplemental S4), indicating that both serine residues are epimerized. ^{48}YLRPPSFLR^{56}, also from the N-terminal region of αB, is 12 ± 1% epimerized in the WI cortex and 15.7% ±0.6% in the WI nucleus. This exceeds the degree of epimerization (2.5% ±0.2%) detected in ^{83}HFSPEELK^{90}, located in the alpha-crystallin domain of αB. In total, serine epimerization is noted for positions 19, 21, 53 and 85 for αB and 20 and 162 for αA. Extensive serine racemization has been detected at both Ser59 and Ser62 in ^{55}TVLDSGISEVR^{65} from αA. By age 40, it was found that ^{55}TVLDSGISEVR^{65} contained 44% D-Ser between these two sites in cataract lenses, compared to only 17% in normal lenses (Hooi et al., 2013). Interestingly, serine epimerization is strongly correlated with loss of solubility, indicating that, while less abundant than aspartic acid isomerization, it may contribute significantly to age-related pathologies associated with the lens.

5. Conclusions

While it is known that long-lived proteins fall victim to various spontaneous degradations as they age in the body, it has been difficult to monitor subtle, yet prolific, modifications such as isomerization and epimerization. By tracking differences between the newly synthesized proteins in the cortex of the lens and the oldest, most highly degraded proteins in the nucleus, we establish the time-course for protein isomerization as a function of influencing factors such as local sequence, tertiary structure, and solubility. Peptides from the cortical fractions were found to lack L-isoAsp, which accumulated significantly in the water-insoluble fractions of the nucleus. PIMT is more prevalent in the cortex than the nucleus, and *in vitro* studies confirm that PIMT activity can account for the observed absence of L-isoAsp. Consequently, isomerization occurs in the cortex but it is actively repaired by PIMT, whereas PIMT activity declines in the nucleus, although isomerization and protein aging continue. Isomerization tendencies can also differ between highly similar proteins, such as αA and αB crystallin. Although αB appears to be less prone to isomerization, αA excels at sustaining damage while remaining soluble and makes a greater contribution towards refractive index. These differences in age-induced isomerization and function may explain why both αA and αB are needed in the lens. In many cases, isomerization appears to facilitate protein aggregation and loss of solubility. Given the long list of age-related diseases where protein aggregation is observed, including cataracts, Alzheimer's, Parkinson's, myofibrillar myopathy, and many others, it is likely that many of the

observations detailed herein will extend to other systems beyond the lens and may offer clues for understanding their pathogenesis.

Supplementary Material

Refer to Web version on PubMed Central for supplementary material.

Acknowledgments

The authors would like to thank Dr. Joseph Horwitz from the Stein Eye Institute at the University of California, Los Angeles for his invaluable advice and expertise on the human eye lens and for donating the trephine for lens separation.

Funding

The authors gratefully acknowledge funding from the National Institutes of Health NIGMS [grant number R01GM107099].

References

Augusteyn RC. Growth of the human eye lens. Mol Vis. 2007; 13:252–7. [PubMed: 17356512]

Chavous DA, Jackson FR, O'Connor CM. Extension of the Drosophila lifespan by overexpression of a protein repair methyltransferase. Proc Natl Acad Sci. 2001; 98:14814–14818. https://doi.org/10.1073/pnas.251446498. [PubMed: 11742076]

Fujii N. D-amino acid in elderly tissues. Biol Pharm Bull. 2005; 28:1585–1589. https://doi.org/10.1248/bpb.28.1585. [PubMed: 16141520]

Fujii, N., Kaji, Y., Fujii, N., Nakamura, T., Motoie, R., Mori, Y., Kinouchi, T. Collapse of homochirality of amino acids in proteins from various tissues during aging. Chem Biodivers. 2010. https://doi.org/10.1002/cbdv.200900337

Fujii N, Sakaue H, Sasaki H, Fujii N. A rapid, comprehensive liquid chromatography-mass spectrometry (LC-MS)-based survey of the Asp isomers in crystallins from human cataract lenses. J Biol Chem. 2012; 287:39992–40002. https://doi.org/10.1074/jbc.M112.399972. [PubMed: 23007399]

Fujii N, Takata T, Fujii N, Aki K. Isomerization of aspartyl residues in crystallins and its influence upon cataract. Biochim Biophys Acta – Gen Subj. 2016; 1860:183–191. https://doi.org/10.1016/j.bbagen.2015.08.001.

Griffith SC, Sawaya MR, Boutz DR, Thapar N, Katz JE, Clarke S, Yeates TO. Crystal structure of a protein repair methyltransferase from Pyrococcus furiosus with its L-isoaspartyl peptide substrate. J Mol Biol. 2001; 313:1103–16. https://doi.org/10.1006/jmbi.2001.5095. [PubMed: 11700066]

Groenen, PJTA., Merck, KB., De Jong, WW., Bloemendal, H. Structure and Modifications of the Junior Chaperone α-Crystallin: From Lens Transparency to Molecular Pathology. Eur J Biochem. 1994. https://doi.org/10.1111/j.1432-1033.1994.00001.x

Hood CA, Fuentes G, Patel H, Page K, Menakuru M, Park JH. Fast conventional Fmoc solid-phase peptide synthesis with HCTU. J Pept Sci. 2008; 14:97–101. https://doi.org/10.1002/psc.921. [PubMed: 17890639]

Hooi MYS, Raftery MJ, Truscott RJW. Age-dependent racemization of serine residues in a human chaperone protein. Protein Sci. 2013; 22:93–100. https://doi.org/10.1002/pro.2191. [PubMed: 23139182]

Hooi MYS, Raftery MJ, Truscott RJW. Racemization of two proteins over our lifespan: Deamidation of asparagine 76 in γS crystallin is greater in cataract than in normal lenses across the age range. Investig Ophthalmol Vis Sci. 2012; 53:3554–3561. https://doi.org/10.1167/iovs.11-9085. [PubMed: 22531704]

Horwitz J, Bova MP, Ding LL, Haley DA, Stewart PL. Lens alpha-crystallin: function and structure. Eye (Lond). 1999; 13(Pt 3b):403–408. https://doi.org/10.1038/eye.1999.114. [PubMed: 10627817]

Horwitz J, Huang QL, Ding L, Bova MP. Lens ?-Crystallin: Chaperone-like properties. Methods Enzymol. 1998; 290:365–383. https://doi.org/10.1016/S0076-6879(98)90032-5. [PubMed: 9534176]

Jia C, Lietz CB, Yu Q, Li L. Site-specific characterization of d-amino acid containing peptide epimers by ion mobility spectrometry. Anal Chem. 2014; 86:2972–2981. https://doi.org/10.1021/ac4033824. [PubMed: 24328107]

Johnson BA, Aswad DW. Enzymatic Protein Carboxyl Methylation at Physiological pH: Cyclic Imide Formation Explains Rapid Methyl Turnover. Biochemistry. 1985; 24:2581–2586. https://doi.org/10.1021/bi00331a028. [PubMed: 4016073]

Lowenson JD, Clarke S. Recognition of D-aspartyl residues in polypeptides by the erythrocyte L-isoaspartyl/D-aspartyl protein methyltransferase. Implications for the repair hypothesis. J Biol Chem. 1992; 267:5985–5995. [PubMed: 1556110]

Lowenson JD, Clarke S. Structural elements affecting the recognition of L-isoaspartyl residues by the L-isoaspartyl/D-aspartyl protein methyltransferase. Implications for the repair hypothesis*. J Biol Chem. 1991; 266:19396–19406. [PubMed: 1833402]

Lund AL, Smith JB, Smith DL. Modifications of the water-insoluble human lens alpha-crystallins. Exp Eye Res. 1996; 63:661–72. https://doi.org/10.1006/exer.1996.0160. [PubMed: 9068373]

Ly T, Zhang X, Sun Q, Moore B, Tao Y, Julian RR. Rapid, quantitative, and site specific synthesis of biomolecular radicals from a simple photocaged precursor. Chem Commun. 2011; 47:2835. https://doi.org/10.1039/c0cc03363d.

Lyon, YA., Sabbah, GM., Julian, RR. Identification of Sequence Similarities among Isomerization Hotspots in Crystallin Proteins. J Proteome Res. 2017. acs.jproteome.7b00073. https://doi.org/10.1021/acs.jproteome.7b00073

Ma Z, Hanson SR, Lampi KJ, David LL, Smith DL, Smith JB. Age-related changes in human lens crystallins identified by HPLC and mass spectrometry. Exp Eye Res. 1998; 67:21–30. https://doi.org/10.1006/exer.1998.0482. [PubMed: 9702175]

Masters PM, Bada JL, Zigler JS. Aspartic acid racemization in heavy molecular weight crystallins and water insoluble protein from normal human lenses and cataracts. Proc Natl Acad Sci U S A. 1978; 75:1204–8. [PubMed: 274711]

McFadden PN, Clarke S. Conversion of isoaspartyl peptides to normal peptides: implications for the cellular repair of damaged proteins. Proc Natl Acad Sci USA. 1987; 84:2595–2599. https://doi.org/10.1073/pnas.84.9.2595. [PubMed: 3472227]

McFadden PN, Clarke S. Protein carboxyl methyltransferase and methyl acceptor proteins in aging and cataractous tissue of the human eye lens. Mech Ageing Dev. 1986; 34:91–105. https://doi.org/10.1016/0047-6374(86)90107-7. [PubMed: 3713272]

McFall-Ngai MJ, Ding LL, Takemoto LJ, Horwitz J. Spatial and temporal mapping of the age-related changes in human lens crystallins. Exp Eye Res. 1985; 41:745–758. https://doi.org/10.1016/0014-4835(85)90183-6. [PubMed: 3830737]

Murray ED, Clarke S. Synthetic peptide substrates for the erythrocyte protein carboxyl methyltransferase. Detection of a new site of methylation at isomerized L-aspartyl residues. J Biol Chem. 1984; 259:10722–10732. [PubMed: 6469980]

Noguchi S. Structural changes induced by the deamidation and isomerization of asparagine revealed by the crystal Structure of Ustilago sphaerogena ribonuclease U2B. Biopolymers. 2010; 93:1003–1010. https://doi.org/10.1002/bip.21514. [PubMed: 20623666]

O'Connor PB, Cournoyer JJ, Pitteri SJ, Chrisman PA, McLuckey SA. Differentiation of aspartic and isoaspartic acids using electron transfer dissociation. J Am Soc Mass Spectrom. 2006; 17:15–19. https://doi.org/10.1016/j.jasms.2005.08.019. [PubMed: 16338146]

Pettersen EF, Goddard TD, Huang CC, Couch GS, Greenblatt DM, Meng EC, Ferrin TE. UCSF Chimera—A Visualization System for Exploratory Research and Analysis. J Comput Chem. 2004; 25:1605–1612. https://doi.org/10.1002/jcc.20084. [PubMed: 15264254]

Qin Z, Dimitrijevic A, Aswad DW. Accelerated protein damage in brains of PIMT+/−mice; a possible model for the variability of cognitive decline in human aging. Neurobiol Aging. 2015; 36:1029–1036. https://doi.org/10.1016/j.neurobiolaging.2014.10.036. [PubMed: 25465735]

Rao PV, Huang Q ling, Horwitz J, Zigler JS. Evidence that α-crystallin prevents non-specific protein aggregation in the intact eye lens. BBA – Gen Subj. 1995; 1245:439–447. https://doi.org/10.1016/0304-4165(95)00125-5.

Riggs, DL., Gomez, SV., Julian, RR. Sequence and Solution Effects on the Prevalence of d -Isomers Produced by Deamidation. ACS Chem Biol acschembio 7b00686. 2017. https://doi.org/10.1021/acschembio.7b00686

Samuel Zigler, J., Goosey, J. Aging of protein molecules: lens crystallins as a model system. Trends Biochem Sci. 1981. https://doi.org/10.1016/0968-0004(81)90050-5

Srinivas P, Narahari A, Petrash JM, Swamy MJ, Reddy GB. Importance of eye lens α-crystallin heteropolymer with 3:1 αA to αB ratio: Stability, aggregation, and modifications. IUBMB Life. 2010; 62:693–702. https://doi.org/10.1002/iub.373. [PubMed: 20836128]

Stephenson RC, Clarke S. Succinimide formation from aspartyl and asparaginyl peptides as a model for the spontaneous degradation of proteins. J Biol Chem. 1989; 264:6164–6170. [PubMed: 2703484]

Tao WA, Zhang D, Nikolaev EN, Cooks RG. Copper(II)-assisted enantiomeric analysis of D, L-amino acids using the kinetic method: Chiral recognition and quantification in the gas phase. J Am Chem Soc. 2000; 122:10598–10609. https://doi.org/10.1021/ja000127o.

Tao Y, Julian RR. Identification of amino acid epimerization and isomerization in crystallin proteins by tandem LC-MS. Anal Chem. 2014; 86:9733–9741. https://doi.org/10.1021/ac502296c. [PubMed: 25188914]

Tao Y, Quebbemann NR, Julian RR. Discriminating d-amino acid-containing peptide epimers by radical-directed dissociation mass spectrometry. Anal Chem. 2012; 84:6814–6820. https://doi.org/10.1021/ac3013434. [PubMed: 22812429]

Truscott, RJW., Friedrich, MG. The etiology of human age-related cataract. Proteins don't last forever. Biochim Biophys Acta. 2016. https://doi.org/10.1016/j.bbagen.2015.08.016

Yamamoto A, Takagi H, Kitamura D, Tatsuoka H, Nakano H, Kawano H, Kuroyanagi H, Yahagi Y, Kobayashi S, Koizumi K, Sakai T, Saito K, Chiba T, Kawamura K, Suzuki K, Watanabe T, Mori H, Shirasawa T. Deficiency in protein L-isoaspartyl methyltransferase results in a fatal progressive epilepsy. J Neurosci. 1998; 18:2063–74. [PubMed: 9482793]

Yi L, Beckley N, Gikanga B, Zhang J, Wang YJ, Chih HW, Sharma VK. Isomerization of Asp-Asp motif in model peptides and a monoclonal antibody fab fragment. J Pharm Sci. 2013; 102:947–959. https://doi.org/10.1002/jps.23423. [PubMed: 23280575]

Zhang J, Yip H, Katta V. Identification of isomerization and racemization of aspartate in the Asp-Asp motifs of a therapeutic protein. Anal Biochem. 2011; 410:234–243. https://doi.org/10.1016/j.ab.2010.11.040. [PubMed: 21130067]

Zhao H, Brown PH, Schuck P. On the distribution of protein refractive index increments. Biophys J. 2011; 100:2309–2317. https://doi.org/10.1016/j.bpj.2011.03.004. [PubMed: 21539801]

Zheng X, Deng L, Baker ES, Ibrahim YM, Petyuk VA, Smith RD, Govind N, Ibrahim YM, Kabanda MM, Dubery IA, Heyman HM, Smith RD, Madala NE, Baker ES, McLean JA. Distinguishing d – and l -aspartic and isoaspartic acids in amyloid ? peptides with ultrahigh resolution ion mobility spectrometry. Chem Commun. 2017; 8:1381–1388. https://doi.org/10.1039/C7CC03321D.

Highlights

- Investigation of crystallin isomerization as a function of age, location within the lens, protein solubility and tertiary structure
- The degree of isomerization is significantly higher in the nucleus than in the cortex
- Protein isoaspartyl methyltransferase may play a critical role in repairing isomerized Asp residues in the cortex
- Sequential Asp residues also serve as isomerization hotspots, especially in αA crystalline
- αB appears to be less prone to isomerization than αA, but is also less capable maintaining solubility upon spontaneous degradation

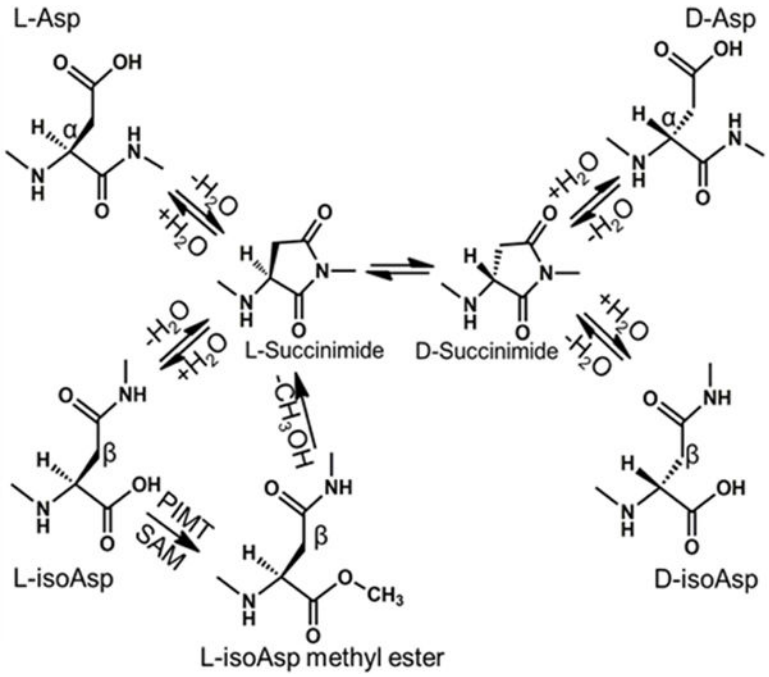

Fig. 1. Spontaneous aspartic acid isomerization via a succinimide intermediate

Alpha and beta carbons are labeled. PIMT conversion of L-isoAsp back to the L-succinimide intermediate via L-isoAsp methyl ester. (After last paragraph of introduction)

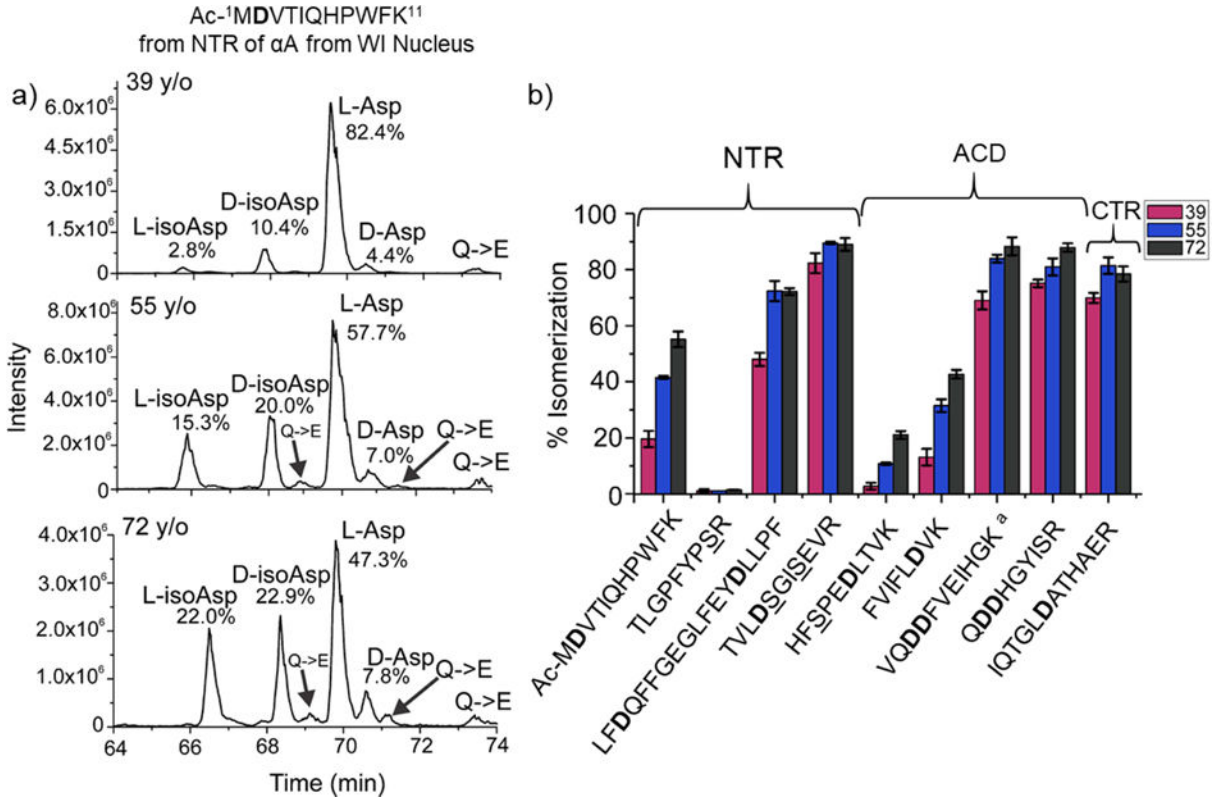

Fig. 2. Results for the changes in isomerization from the WI nuclei of the 39, 55 and 72-year-old lenses

a) LC chromatograms of Ac-MDVTIQHPWFK, from the WI nucleus of each age. Glutamine deamidation is labeled Q→E. b) Compilation of the percent isomerization per peptide. Aspartic acid and serine residues are bold and underlined, respectively. NTR= N-terminal region, ACD= alpha-crystallin domain and CTR= C-terminal region. [a]Minimum percent isomerization for peptides where L-Asp coelutes with another isomer. Error bars represent standard deviation of technical triplicates.

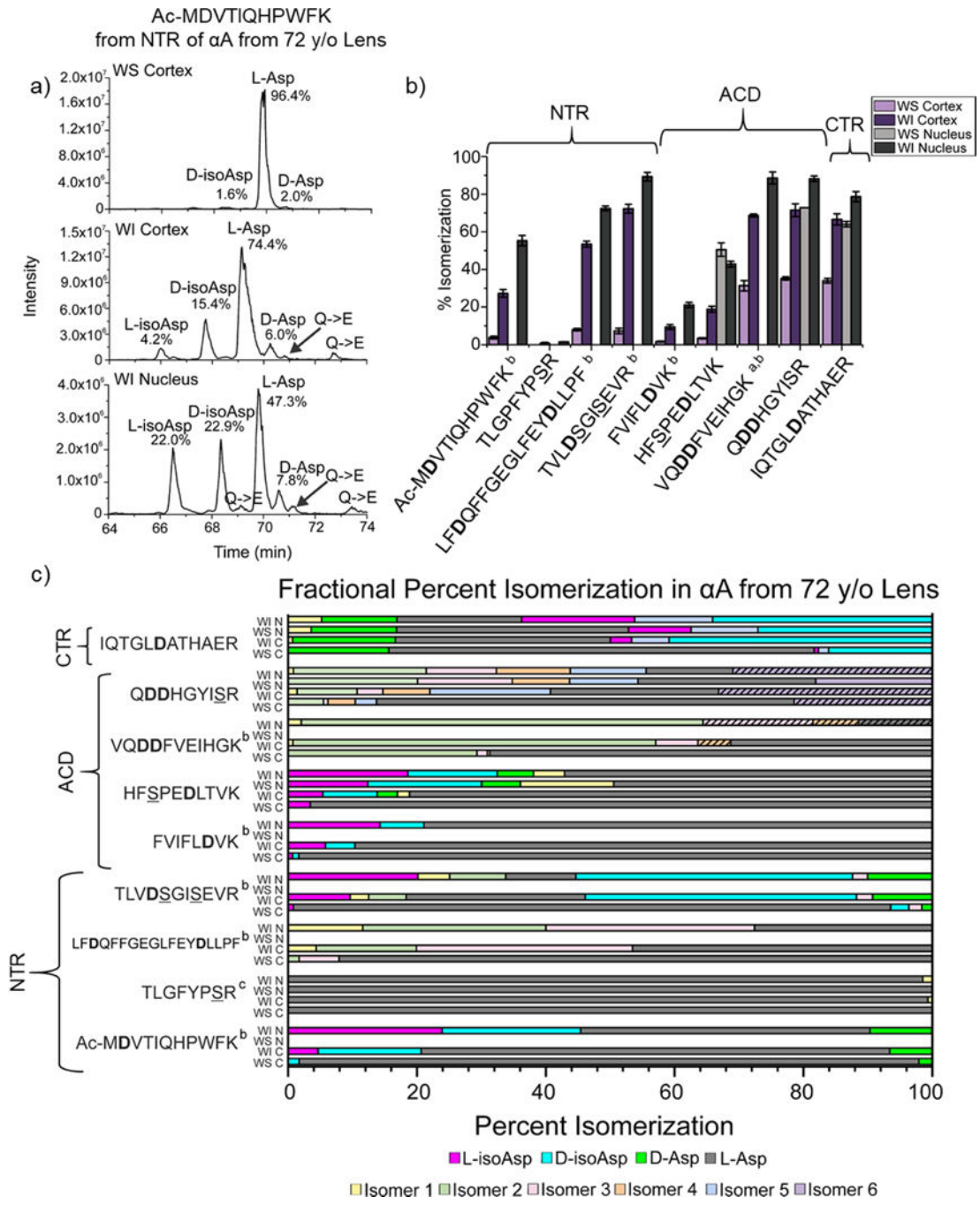

Fig. 3. Results for αA from the 72-year-old lens. a) LC chromatograms for Ac-MDVTIQHPWFK b) Compilation of the percent isomerization per peptide. Format is similar to Fig. 2b. [a]Minimum percent isomerization for peptides where L-Asp coelutes with another isomer. [b]Insufficient ion count for analysis of the peptide from the WS nucleus. [c]Peptide containing serine epimers, gray bar represents L-Ser. c) Fractional percent isomerization for each peptide. The first line in the legend contains isomers with known identities, and the second line unknown isomers. Red asterisk indicates serine isomerization. Black diagonal stripes represent co-eluting species.

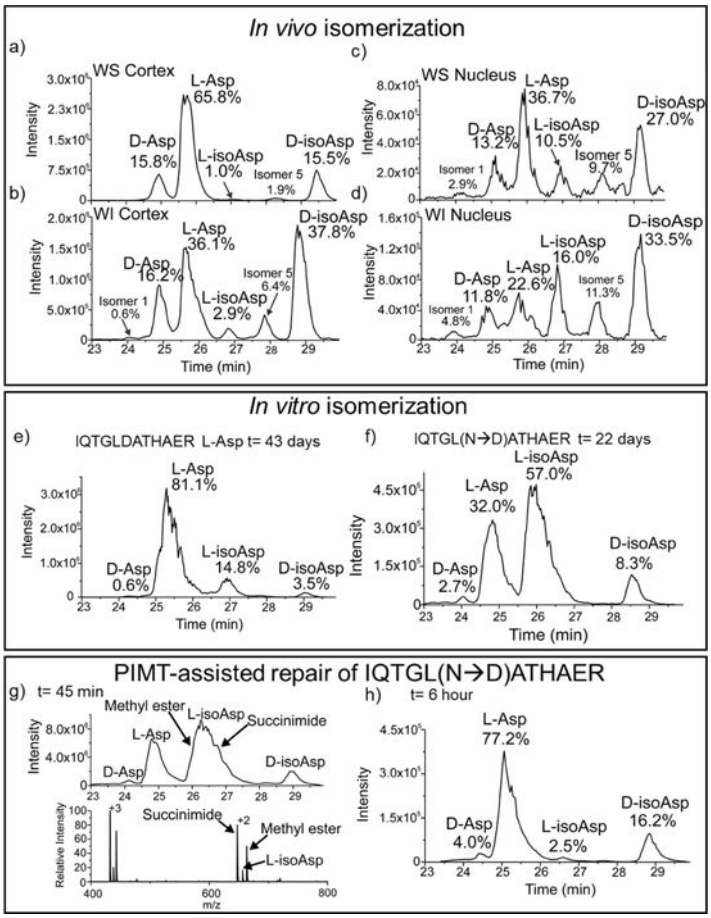

Fig. 4. Differences between *in vivo* versus *in vitro* IQTGLDATHAER isomerization products

a-d) IQTGLDATHAER chromatograms from the WS cortex, WI cortex, WS nucleus and WI nucleus from the 72 -year-old lens. e) *in vitro* isomerization of the IQTGLDATHAER L-Asp synthetic peptide. f) *in vitro* isomerization products emerging from the deamidation of a synthetic peptide IQTGL(N→D)ATHAER after 22 days. g) Products from the PIMT treatment of IQTGLDATHAER after 45 minutes. Mass spectrum on bottom shows that the succinimide and methyl ester intermediates coelute with L-isoAsp. h) Extracted ion chromatogram of IQTGLDATHAER after 6 hours of incubation with PIMT

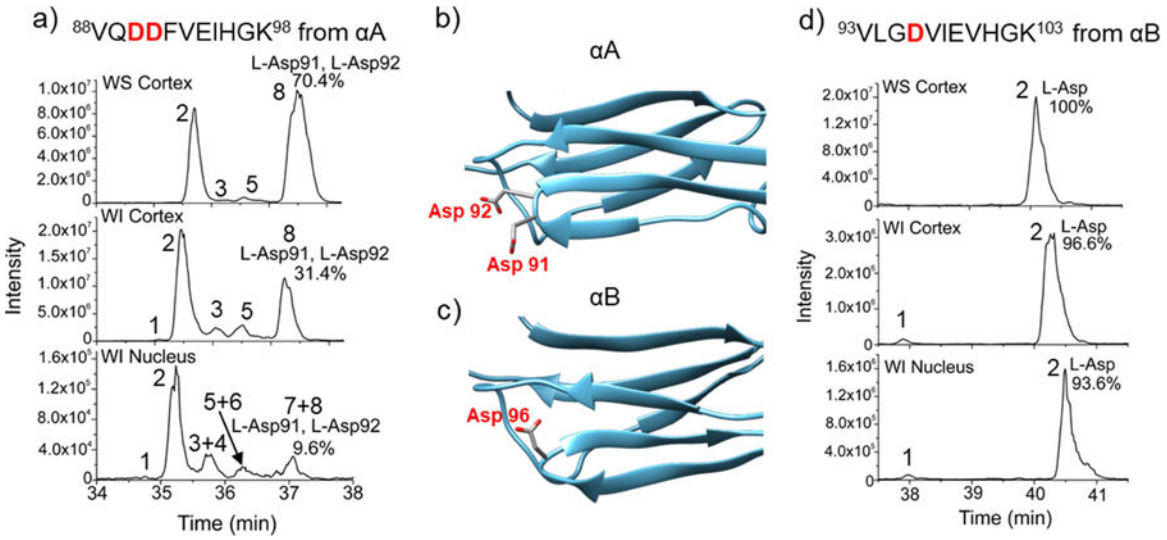

Fig. 5. Asp-Asp isomerization hotspot in αA Crystallin

a) LC chromatogram of ^{88}VQDDFVEIHGK^{98} from the WS cortex, WI cortex and WI nucleus of the 72 -year-old lens. Peaks are labeled 1-8, where peak #8 was identified as L-Asp91,L-Asp92. b,c) Highlighted region of αA and αB where this motif is present. Crystal structure of bovine αA (PDB ID: 3LIF) (34). Crystal structure of human αB (PDB ID: 3L1G) (34). d) LC chromatogram of ^{93}VLGDVIEVHGK^{103} from the WS cortex, WI cortex and WI nucleus of the 72-year-old lens. Both peaks are labeled, and peak #2 was identified as L-Asp.

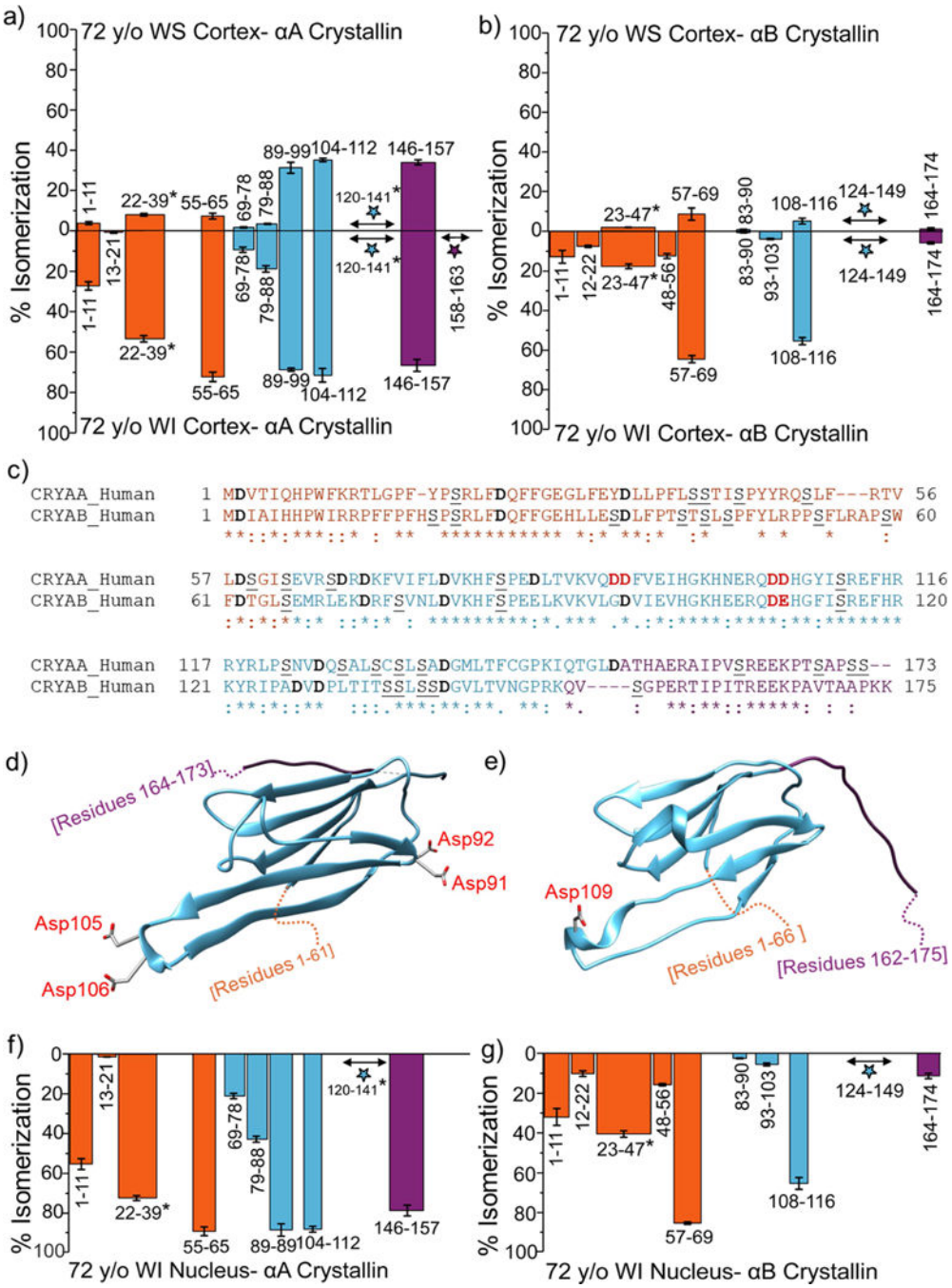

Fig. 6. Changes in isomerization between αA and αB in the 72 -year-old lens

a,b) Degree of isomerization in αA and αB from 72 -year-old WS cortex. Each tryptic peptide is numbered according to position in the protein, and colored based on structural motif. Orange= N-terminal region (NTR), blue= alpha-crystallin domain (ACD) and purple= C-terminal region (ACD). Sites, where isomerization was detected but could not be identified, are represented as stars. c) Amino acid sequences of αA and αB color coded based on structural motif. Aspartyl residues are in bold, black text. Serine residues are in underlined, black text. Acidic amino acid repeats are in bold, red text. d) Crystal structure of

bovine αA (PDB ID: 3LIF). e) Crystal structure of human αB (PDB ID: 3L1G). f,g) Degree of isomerization in αA and αB from 72 -year-old WI nucleus. Identical formatting to Fig. 6a,b. Asterisks next to peptide numbers denote non-tryptic peptides.